J. Phys.: Condens. Matter **21** (2009) 124210 (6pp) doi:10.1088/0953-8984/21/12/124210

Structural transitions in $RNi_{10}Si_2$ intermetallics

O Moze[1], W A Kockelmann[2], M Hofmann[3], J M Cadogan[4], D H Ryan[5] and K H J Buschow[6]

[1] Dipartimento di Fisica, Università di Modena e Reggio Emilia, via G. Campi 213/a, 41100, Modena, Italy
[2] ISIS Facility, Rutherford Appleton Laboratory, Didcot OX11 0QX, UK
[3] Technische Universität München, ZBE FRM-II, 85747 Garching, Germany
[4] Department of Physics and Astronomy, University of Manitoba, Winnipeg, MB, R3T2N2, Canada
[5] Physics Department, McGill University, Montreal, H3A2T8, Canada
[6] Van der Waals–Zeeman Institute, Universiteit van Amsterdam, 1018 XE, The Netherlands

E-mail: oscar.moze@unimore.it

Received 16 October 2008, in final form 28 November 2008
Published 25 February 2009
Online at stacks.iop.org/JPhysCM/21/124210

Abstract

Intermetallic compounds of the type $RFe_{10}Si_2$ and $RCo_{10}Si_2$ crystallize in the $ThMn_{12}$ structure (space group $I4/mmm$) whilst the heavy rare earth series $RNi_{10}Si_2$ crystallize in a maximal subgroup of $I4/mmm$, $P4/nmm$. Reported here are neutron powder diffraction investigations for $TbNi_{10}Si_2$ and $ErNi_{10}Si_2$ which show that the $P4/nmm$ structure undergoes a high temperature order–disorder phase transition at approximately 930 °C above which the ordered Ni and Si fractions revert to a random distribution on 4d and 4e sites. The volume expansion has been tracked in detail via the temperature dependence of the lattice parameters, whilst the temperature dependence of the thermal expansion coefficients α_{11}, α_{33} and α_{volume} has been determined from the lattice parameters. Associated with the order–disorder transition is a transition associated with a displacement of the R ion along the c-axis. Both transitions are of second order and the critical exponent associated with the order–disorder and displacive transitions, $\beta = 0.31$, is in excellent agreement with the exponent determined for the three-dimensional Ising model.

(Some figures in this article are in colour only in the electronic version)

1. Introduction

Ternary rare earth (R) intermetallic compounds with compositions of the type $RT_{12-x}M_x$ where T is a 3d transition metal (T = Fe, Co, Ni, Mn) and M a stabilizing element such as Ti, V, Al, Ga and Si form an important class of materials which have been extensively investigated in the recent past [1–4]. Compounds based on R = Sm and T = Fe are of particular pertinence, since they have good performance criteria as permanent magnets i.e. high magnetic ordering temperatures combined with a large saturation magnetization and similarly large uniaxial magnetic anisotropy. Of particular pertinence is the site occupation of the stabilizing element in the aforementioned compounds. This site occupancy plays a fundamental role in determining the magnetic and structural properties for this series. For the $ThMn_{12}$ [5] (space group $I4/mmm$) in which the $RT_{12-x}M_x$ series crystallize, the transition metal and metalloid elements have the possibility of occupying three sites, 8i (x, 0, 0, $x \sim 0.35$), 8j (x, $\frac{1}{2}$, 0, $x \sim 0.27$) and 8f ($\frac{1}{4}$, $\frac{1}{4}$, $\frac{1}{4}$). The preferential occupation of the T and M atoms on any of these sites, as well as the magnetic structure of the constituent magnetic sublattices, has been systematically characterized by neutron diffraction for a large number of R–T–M (T = Fe, Co, Mn) compounds of the type $RT_{12-x}M_x$, ($1 < x < 6$), which crystallize in the $ThMn_{12}$ structure. Therefore a great deal is now known about the mixing of T and M elements on the 8i, 8j and 8f sites. Examples which have appeared in the literature are Y–Fe–Ti [6], Y–Fe–V [7], Y–Fe–Al [8], R–Mn–Al [9], R–Co–V [10, 11], Y–Co–Ti [12],

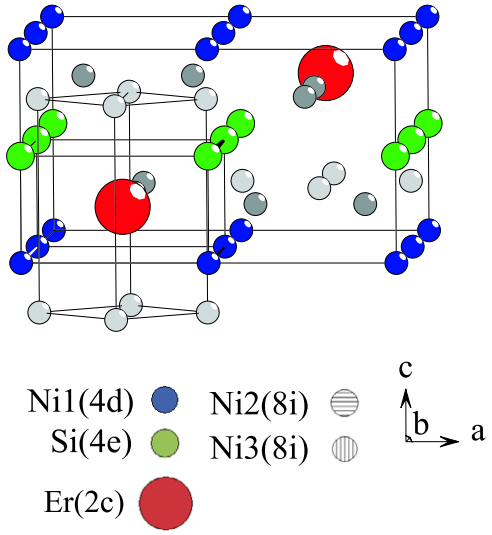

Figure 1. Crystal structure of $RNi_{10}Si_2$ compounds (space group $P4/nmm$).

Table 1. Structural parameters for $RNi_{10}Si_2$ compounds which crystallize in space group $P4/nmm$. R–X is the shortest interatomic distance to the rare earth site. Parameters in *italics* refer to sites in space group $I4/mmm$. The origin of the unit cell in $P4/nmm$ has been shifted by (1/4, 1/4, 1/4) with respect to $I4/mmm$. Numerical values in the table are those for $TbNi_{10}Si_2$ at room temperature.

		$a = 8.1965$ Å	$c = 4.667$ Å	
	x/a	y/a	z/c	R–X (Å)
R (2c)	1/4	1/4	0.2255	
R(2a)	*0*	*0*	*0*	
Ni_1 (8i)	0	0.6043	0.2379	2.9042
Ni_1 (8i)	*$x, x \sim 0.35$*	*0*	*0*	*2.9016*
Ni_2 (8i)	0	0.0254	0.7298	2.9566
Ni_2 (8i)	*0*	*0*	*0*	*2.9710*
Ni_3 (4d)	0	0	0	3.0832
Ni_3 (8f)	*1/4*	*1/4*	*1/4*	*3.1242*
Si (4e)	0	0	1/2	3.1684
Si (8f)	*1/4*	*1/4*	*1/4*	*3.1242*

Y–Co–Mo [12], Y–Fe–Cr [13], R–Co–Mo [14], R–Fe–Ga [15], R–Fe–Mo [16], R–Fe–Ta [17, 18], R–Fe–Mn [19].

For compounds with Fe and Co sublattices, the R and T sublattices are generally magnetic, with the R sublattice being polarized by the strong R–T exchange interaction. A prominent example of where the transition metal sublattice is known to be non-magnetic (or possibly very weakly magnetic) is the case of the series $RNi_{10}Si_2$ [20, 21]. The fact that the Ni sublattice does not order magnetically in similar compounds has rendered these materials less interesting from an applications point of view. The Ni–Si site occupancies for $YNi_{10}Si_2$, as determined by neutron diffraction [22], showed a marked preference of Si for the 8i site, with some small residual occupancy of Si on the 8j and 8f sites. A similar Si site occupancy was also observed for $YFe_{10}Si_2$ [23]. A more detailed characterization of the crystal and magnetic structures for the heavy rare earth series $RNi_{10}Si_2$ (R = Tb, Dy, Ho, Er and Tm) [24] revealed that the R sublattice orders only at low cryogenic temperatures (the corresponding series with the light rare earths do not exist). A particular structural characteristic which has rendered this series of interest is that these compounds crystallize in an ordered variant of the $ThMn_{12}$ structure, in the space group $P4/nmm$ (figure 1).

There is an ordered 1:1 distribution of Ni and Si on sites 4d end 4e, and this corresponds to a modulation vector [001] with respect to space group $I4/mmm$. This is a unique feature of rare earth intermetallics of the type $RT_{12-x}M_x$ with T = Ni, which generally crystallize in the $ThMn_{12}$ structure. The general richness and complexity of magnetic interactions in rare earth intermetallics which crystallize in the $ThMn_{12}$ structure is reflected in extremely complex magnetic structures of both rare earth and Fe sublattices for the series $R(R = Dy, Ho)Fe_4Al_8$ [25], $M(M = Lu, Y)Fe_4Al_8$ [26].

In this paper we report on neutron powder diffraction measurements of the temperature dependence for Ni and Si fractions on 4d and 4e sites and the critical exponent associated with the order–disorder transition, as well as the temperature dependence and associated critical exponent for the displacement of the R ion. These measurements demonstrate that neutron diffraction, and in particular neutron powder diffraction, is now a well demonstrated and unique probe of atomic disorder phenomena in metals and intermetallics.

2. Experiment

Samples with nominal compositions $RNi_{10}Si_2$ (R = Tb, Er) and weight of approximately 10 g were prepared by arc melting, under an atmosphere of Ar gas, constituent materials of at least 3 N purity. These were then annealed at 1050 °C for 3 days under Ar. X-ray diffraction confirmed that the compounds do indeed order in space group $P4/nmm$, a subgroup of $I4/mmm$.

Neutron diffraction measurements were carried out in the temperature range from 0 to 1100 °C using the energy dispersive time-of-flight neutron diffractometer ROTAX, located at the neutron spallation source ISIS, Rutherford Appleton Laboratory, UK. Each diffraction pattern was corrected for linear absorption and analysed using the GSAS Rietveld refinement code [27]. Parameters that were refined included: lattice constants, isotropic temperature factors, atomic site coordinates and Ni, Si occupancies on the 4d and 4e sites. The following neutron scattering lengths were used: $b_{Tb} = 7.38$ fm, $b_{Er} = 7.79$ fm, $b_{Ni} = 10.34$ fm, $b_{Si} = 4.15$ fm. The large contrast between the neutron scattering lengths for Ni and Si is particularly advantageous in the present study, since the site occupancies of these atoms can be determined with a high degree of precision.

3. Results and analysis

Rietveld profile refinements of the diffraction patterns were carried out on the basis of structural parameters as reported in table 1. The space group in which the heavy rare earth

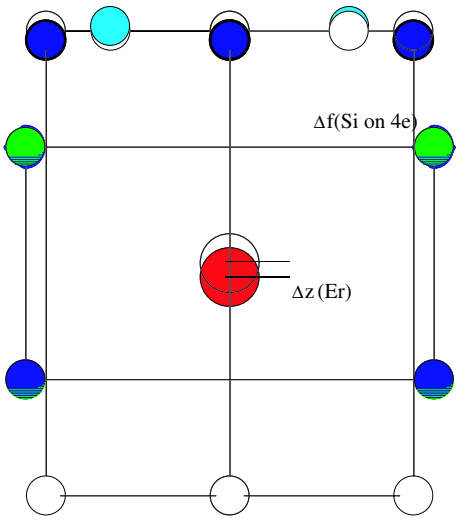

Figure 2. Schematic of the atomic displacement phase transition in $RNi_{10}Si_2$ compounds, as viewed in the a–b plane.

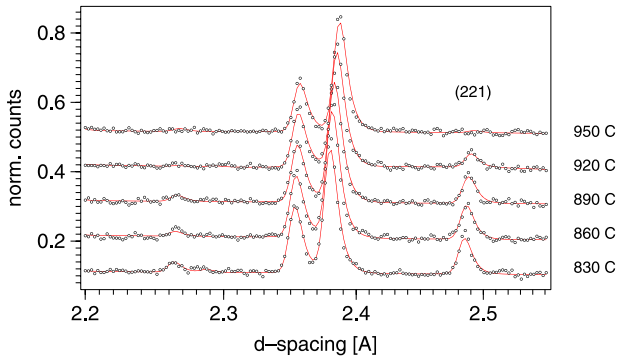

Figure 3. Sections of neutron diffraction patterns for $ErNi_{10}Si_2$.

series of $RNi_{10}Si_2$ compounds crystallize is a maximal non-isomorphic subgroup of $I4/mmm$. In particular, the 8f site of the parent space group $I4/mmm$ is split into 4d and 4e sites in $P4/nmm$. These sites are occupied by Ni and Si respectively and result in fully ordered distributions of Ni and Si on these sites, respectively. These distributions change with temperature, resulting in a second order transition at a critical temperature above which both 4d and 4e sites are randomly occupied by Ni and Si. Measurements were performed for both warming up and cooling down cycles with no hysteresis effects observed, indicating a smooth second order structural transition.

A stacking of alternating planes of Ni and Si along the c-axis corresponds to a modulation vector of [001]. This stacking was directly verified in the indexing of the observed reflections, indexed by the selection rule for the body centred $ThMn_{12}$ structure $h + k + l = 2n$ together with weaker superstructure reflections which are indexed with a vector [001]. Another prominent feature observed in the present investigation, displayed schematically in figure 2, is a significant displacement of the R atom along the c-direction, away from the special position of the 2a site in the $ThMn_{12}$ structure.

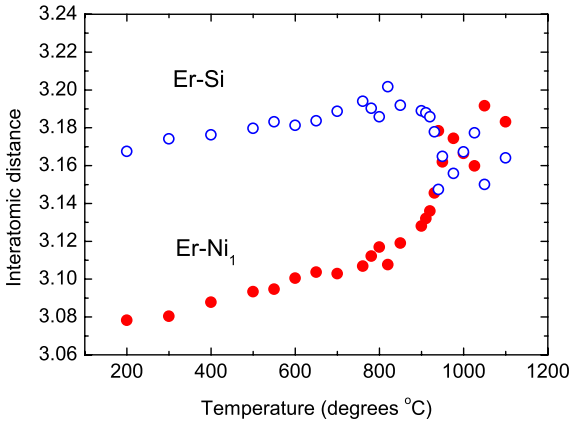

Figure 4. Temperature dependence of the refined values for Er–Si and Er–Ni_1 interatomic distances (in Å) in $ErNi_{10}Si_2$.

A section of the refined diffraction pattern between 830 and 950 °C for $ErNi_{10}Si_2$ is displayed in figure 3. The superstructure reflection (221) has a notable temperature dependence reflecting an increasing disorder on the Ni and Si sites. Associated with the order–disorder transition is a marked variation with temperature in R–Ni interatomic distances, particularly at and near the transition temperature (figure 4). The most significant result of the refinement of the diffraction data is the temperature dependence of the Ni/Si occupancies on 4d and 4e sites together with the temperature dependence of the displacement of the R ion along the c-axis. The dependence of these two order parameters η_{site} and $\eta_{\text{displacement}}$ with temperature T, was fitted to the equation:

$$\eta = K[1 - (T/T_c)^{\epsilon}]^{\beta} \tag{1}$$

where K and ϵ are fitting parameters not related to the phase transition whilst β is the critical exponent associated with the phase transition which occurs at the critical temperature T_c. The two order parameters have been defined as:

$$\begin{aligned} \eta_{\text{site}} &= \Delta f = f - \tfrac{1}{2} \\ \eta_{\text{displacement}} &= \Delta z = \tfrac{1}{2} - z_{\text{Er}} \end{aligned} \tag{2}$$

where f is the Si occupancy on the 4e site.

The resulting fits for the temperature dependence of the order parameters and their associated critical exponents for $ErNi_{10}Si_2$ are displayed in figures 5 and 6 respectively and table 2. As discussed above, both transitions are of second order with no observable hysteresis effects. A further relevant property obtained from the present diffraction data were the thermal expansion coefficients, of which there are three for tetragonal crystal symmetry: α_{11}, α_{33} and the coefficient associated with the volume expansion, α_{vol} [28]. Their temperature dependence was calculated directly from the temperature dependence of the tetragonal lattice parameters $a(T)$ and $c(T)$ and the following expressions for the thermal

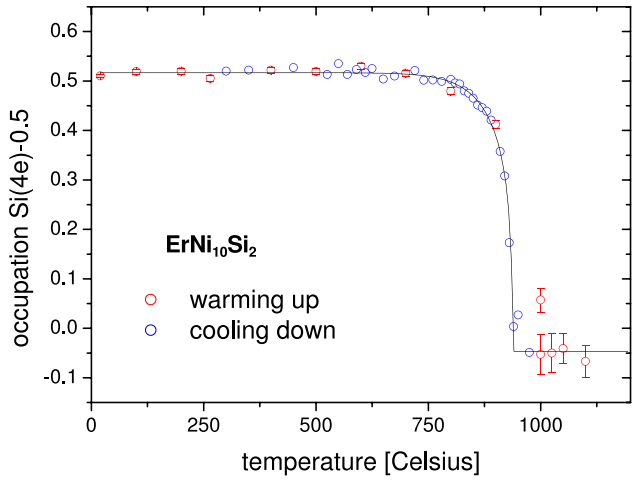

Figure 5. Thermal variation of the order–disorder parameter for $ErNi_{10}Si_2$. The solid line is the fit obtained using equation (1).

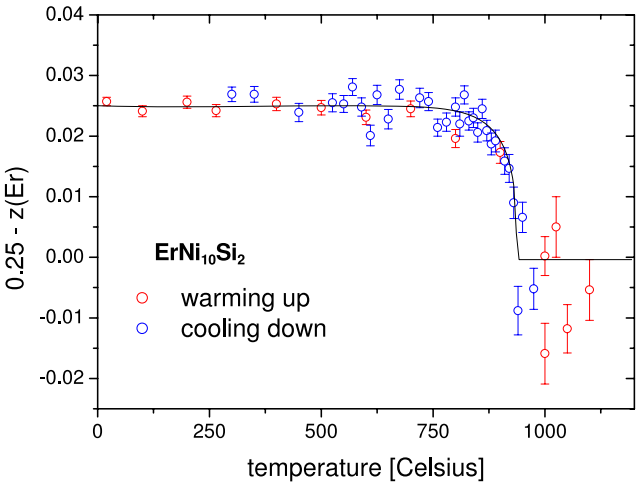

Figure 6. Thermal variation of the order parameter for the displacive phase transition in $ErNi_{10}Si_2$. The solid line is the fit obtained using equation (1).

expansion coefficients:

$$\alpha_{11} = \frac{1}{a(T)}\frac{\mathrm{d}a}{\mathrm{d}T}$$
$$\alpha_{33} = \frac{1}{c(T)}\frac{\mathrm{d}c}{\mathrm{d}T} \qquad (3)$$
$$\alpha_{\mathrm{vol}} = 2\alpha_{11} + \alpha_{33}.$$

The temperature dependence of the lattice parameters for $ErNi_{10}Si_2$ is displayed in figure 7. In order to calculate the thermal expansion coefficients, the functional dependence of the lattice parameters with temperature was in turn fitted to expressions of the form:

$$a(T) = a_0 + a_1 T + a_2 T^2 + a_3 T^3 + \frac{a_4}{1 + \exp[a_5(T - a_6)]}. \qquad (4)$$

This type of expression gives an adequate analytical description for the temperature dependence of the lattice

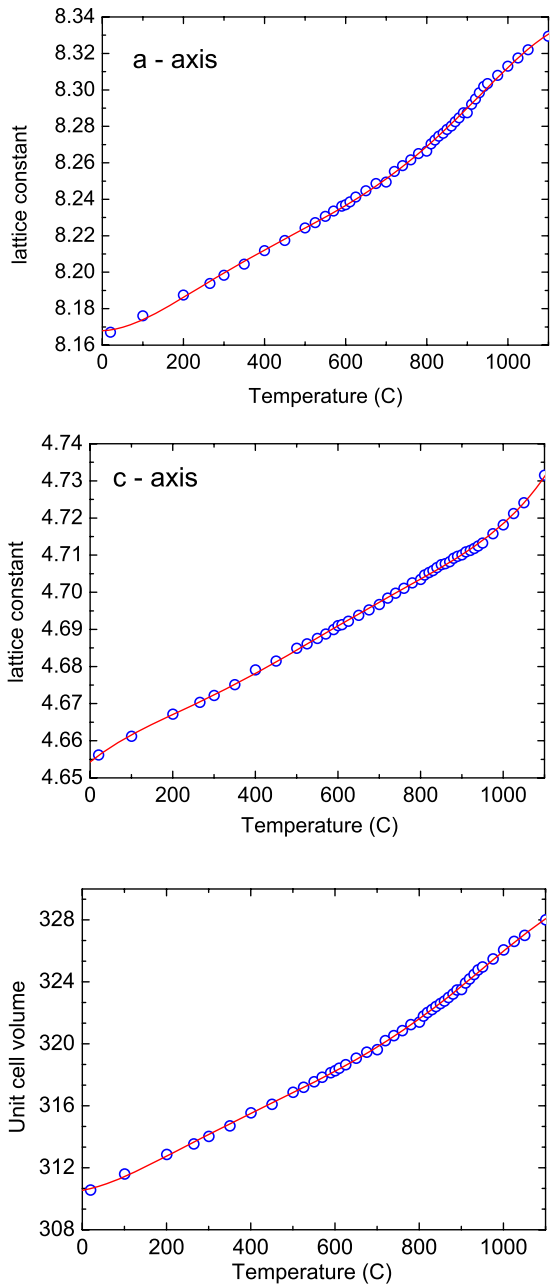

Figure 7. Temperature dependence of the lattice parameters (in Å) and unit cell volume (in $Å^3$) for $ErNi_{10}Si_2$. Lines are results of fits to the data using equation (4).

parameters over an extended temperature range in both the ordered and disordered phases. The calculated temperature dependence of the thermal expansion coefficients for $ErNi_{10}Si_2$ is displayed in figure 8. The structural transitions, together with the fact that they are of second order, are also clearly evidenced in the thermal expansion data.

4. Discussion and conclusion

The value of the critical exponent β for the order–disorder and displacive transitions observed here for these complex multi-sublattice intermetallic compounds is in excellent accord with

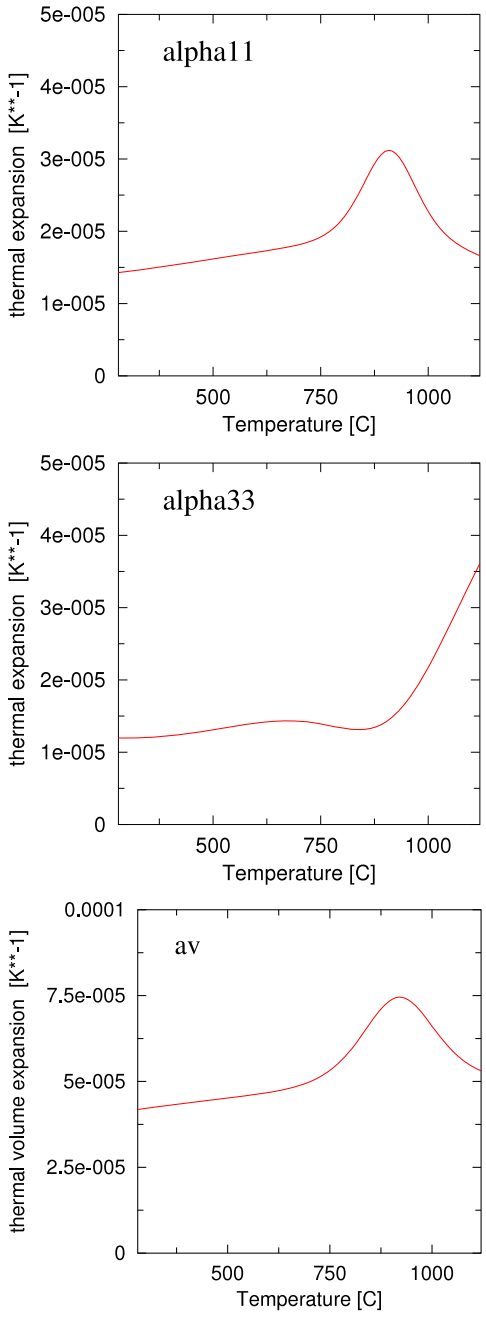

Figure 8. Temperature dependence of the thermal expansion coefficients α_{11}, α_{33} and α_{volume} for $ErNi_{10}Si_2$.

the theoretical predictions of the Renormalization Group and in particular with that calculated from the compressible 3d-Ising model [29]. The observed critical exponent for the atomic order–disorder transition in β-Brass has the same value as that observed in the present investigation for the second order order–disorder transition on 4d and 4e sites [30–32].

The particular structural aspect observed here for the heavy rare earth series of $RNi_{10}Si_2$ compounds sets this series apart from an enormous class of intermetallic compounds of the type $RT_{12-x}M_x$ which are usually observed to crystallize in the $ThMn_{12}$ structure. It would be of interest to characterize more closely in future the structural details of any new compounds of the type and also to model on a more theoretical basis the nature of the $I4/mmm \Longleftrightarrow P4/nmm$ transition via calculations of the lattice dynamics and lattice stability for the $RT_{12-x}M_x$ series for these two respective space groups.

Table 2. Critical exponent β for the order–disorder and atomic displacement transitions for $TbNi_{10}Si_2$ and $ErNi_{10}Si_2$ as determined by neutron diffraction, together with the critical exponent for the long range order parameter as calculated from the compressible 3d-Ising model for β-Brass [29–32]. Tabulated also are the critical temperatures associated with the O–D (order–disorder) and displacive transitions. The fitted value of the parameter ϵ as defined in equation (1) was $\epsilon \sim 14$ for both transitions.

	$\beta_{\text{O-D}}$	β_{displ}	$T_c^{\text{O-D}}$	T_c^{displ}
$TbNi_{10}Si_2$	0.31	0.31	931.8	931.8
$ErNi_{10}Si_2$	0.31	0.31	936.2	936.2
Compressible 3d-Ising	0.31			

Acknowledgments

The authors gratefully acknowledge provision of neutron beam time by ISIS. Financial support for W A Kockelmann and the ROTAX instrument under project 03KLE8BN by the German BMBF is also gratefully acknowledged. J M Cadogan acknowledges support under the Canada Research Chairs scheme.

References

[1] Buschow K H J 1991 *J. Magn. Magn. Mater.* **100** 79
[2] Li H and Coey J M D 1992 *Handbook of Magnetic Materials* vol 6, ed K H J Buschow (Amsterdam: North-Holland) p 1
[3] Suski W 1996 *Handbook on the Physics and Chemistry of Rare Earths* vol 22, ed K A Gschneidner Jr, J C Bunzli and V K Pecharsky (Amsterdam: North-Holland) p 143
[4] Franse J J M and Radwanski R J 1996 *Rare-Earth Permanent Magnets* ed J M D Coey (Oxford: Clarendon) p 143
[5] Florio J V, Rundle R E and Snow A I 1952 *Acta Crystallogr.* **5** 449
[6] Moze O, Pareti L, Solzi M and David W I F 1988 *Solid State Commun.* **66** 465
[7] Solzi M, Pareti L, Moze O and David W I F 1988 *J. Appl. Phys.* **64** 5084
[8] Moze O, Ibberson R M and Buschow K H J 1990 *J. Phys.: Condens. Matter* **2** 1677
[9] Moze O, Ibberson R M, Caciuffo R and Buschow K H J 1990 *J. Less-Common Met.* **166** 329
[10] Moze O, Ibberson R M and Buschow K H J 1993 *Solid State Commun.* **196** L1–2
[11] Rao G H, Liu W F, Huang Q, Ouyang Z W, Wang F W, Xiao Y G, Lynn J W and Liang L K 2006 *Phys. Rev.* B **71** 144430
[12] Moze O, Pareti L and Buschow K H J 1995 *J. Phys.: Condens. Matter* **7** 7981
[13] Moze O and Buschow K H J 1995 *J. Alloys Compounds* **233** 165
[14] Moze O and Buschow K H J 1995 *Z. Phys.* B **101** 521
[15] Moze O, Cadogan J M, Janssen Y, de Boer F R, Buschow K H J and Kennedy S J 2001 *Eur. J. Phys.* B **23** 29
[16] Ayres de Campos J, Ferreira L P, Cruz M M, Gil J M, Mendes P J, Ferreira I C, Bacmann M, Soubeyroux J L, Fruchart D, Godinho M and Ayres de Campos N 1999 *J. Phys.: Condens. Matter* **11** 687

[17] Cadogan J M, Ryan D H, Swainson I P and Gagnon R 1999 *J. Phys.: Condens. Matter* **11** 8975
[18] Piquer C, Palacios E, Artigas M, Bartolomé J, Rubin J, Campo J and Hofmann M 2000 *J. Phys.: Condens. Matter* **12** 2265–78
[19] Morales M, Bacmann M, Wolfers P, Fruchart D and Ouladdiaf B 2001 *Phys. Rev.* B **64** 144426
[20] Stefanski P, Suski S, Wochowski K and Mydlarz T 1996 *Solid State Commun.* **97** 465
[21] Tang H, Qiao G W, Liu J P, Sellmyr D J, de Boer F R and Buschow K H J 2001 *J. Phys.: Condens. Matter* **117** 565
[22] Moze O, Ibberson R M and Buschow K H J 1991 *Solid State Commun.* **78** 473
[23] Buschow K H J 1988 *J. Appl. Phys.* **63** 3130
[24] Kockelmann W, Hofmann M, Moze O, Kennedy S J and Buschow K H J 2002 *Eur. J. Phys.* **30** 25
[25] Paixão J A, Sørensen S Aa, Lebech B, Lander G H, Brown P J, Langridge S, Talik E and Gonçalves A P 2000 *Phys. Rev.* B **61** 6176–88
[26] Paixão J A, Ramos Silva M, Waerenborgh J C, Gonçalves A P, Lander G H, Brown P J, Godinho M and Burlet P 2001 *Phys. Rev.* B **63** 054419
[27] Larson A C and von Dreele R B 1984 *General Structure Analysis System (GSAS)* LAUR 86-748
[28] Paufler P and Weber T 1999 *Eur. J. Mineral.* **11** 721–30
[29] Papon P, Leblond J and Meijer P H E 2002 *The Physics of Phase Transitions: Concepts and Applications* (Berlin: Springer) p 241
[30] Chipman D R and Walker C B 1972 *Phys. Rev.* B **5** 3823–31
[31] Baker G A and Essam J W 1970 *Phys. Rev. Lett.* **4** 447
[32] Baker G A and Essam J W 1971 *J. Chem. Phys.* **55** 861